Structure-Property Relationships in *Arapaima Gigas* Scales Revealed by Nanoindentation Tests

F.G. Torres[1,*], E. Le Bourhis[2,*], O.P. Troncoso[1], and J. Llamoza[1]
[1]Department of Mechanical Engineering, Pontificia Universidad Católica del Perú, Lima 32, Peru
[2]Institut P', CNRS - Université de Poitiers – ENSMA - UPR 3346, SP2MI-Téléport 2-Bd Marie et Pierre Curie, B.P. 30179, 86962 Futuroscope-Chasseneuil Cedex, France

Received: 5 June 2013, Accepted: 5 August 2013

SUMMARY

Fish scales from *Arapaima Gigas* have been studied in terms of their structure (morphology, collagen content) and mechanical properties. A strong mechanical gradient was revealed in the scale, hardness and reduced modulus being reduced by a factor of three. Correlations between the hardness and reduced modulus and the mineral content have been found. The external mineral rich layers were determined to be hard and stiff while the inner surface, being collagen rich, was less hard and less stiff. The inside of the scales showed a progressive decrease of mechanical properties, with variations attributed to the plywood-like structure of the scale.

Keywords: Arapaima Gigas scales, Plywood structure, Collagen content, Nanoindentation response

1. INTRODUCTION

Fish scales are hard skeletal elements composed of a mineral phase of calcium-deficient hydroxyapatite and an extracellular matrix, mainly closely packed type I collagen fibres, forming a plywood-like structure[1].

Scales provide a flexible and protective outer layer on the dermis of a large variety of fish[2]. The arrangement of fish scales provides a flexible skin that allows for changes in shape[3]. Currey has reported that some fish scales are so tough that they cannot be easily fractured even after immersion in liquid nitrogen[4]. In addition, it has been shown that the ridges and grooves on the surface of some fish scales may reduce the swimming drag forces[5].

Browning *et al*. have used macroscale prototypes and finite element based micromechanical models to measure the mechanical response of fish scales to blunt and penetrating indentation loading[6]. They found that the deformation mechanisms of scale bending, scale rotation, tissue shear, and tissue constraint governed the ability of the composite to protect the underlying substrate.

The microstructure and mechanical properties of fish scales have been reported in the past. Ikoma *et al*. studied the properties and structure of fish scales from Pagrus major[7]. They found that the fish scale of Pagrus major had an orthogonal plywood structure of stratified lamellae consisting of closely packed collagen fibres.

Garrano *et al*. have evaluated the mechanical behaviour of fish scales from *Cypinus carpio*[8]. They used scales from three different positions about the body (head, mid-length and tail) and with different moisture contents (from hydrated to fully dehydrated). They found significant differences in properties as a function of anatomical position and hydration.

Another study investigated the spatial distribution of structure, chemical composition and mechanical properties in mineralized fish scales of the species *Atractosteus spatula*. Microindentation and nanoindentation tests were used to assess mechanical properties of samples[9]. Scales from other species such as Moronesaxatilis[3], Ditrematemminck, Sebastesinermis, Mustelusmanago[5] have also been examined.

Torres *et al*. first characterized the fish scales of Arapaima Gigas[10]. They reported the Young modulus of dry and humid scales, the absorption and desorption properties as well as the XRD and FTIR spectra. Also, they showed that the mechanical behaviour of *Arapaima Gigas* scales is similar to that of a laminated composite material.

*Corresponding authors: fgtorres@pucp.edu.pe, eric.le.bourhis@univ-poitiers.fr

Their stress-strain curves present several peaks related to the breakage of successive lamellae.

As with all biological materials, the moisture content plays a role in the mechanical properties of *Arapaima Gigas* scales. In a first study[10], Torres *et al*. measured the maximum tensile strength and Young's modulus of dry *Arapaima Gigas* scales to be 53.86 MPa and 1.38 GPa, respectively while the maximum tensile strength and the Young's modulus of humid scales were 22.26 MPa and 0.83 GPa, respectively. Moreover, in a later study, differential scanning calorimetry (DSC) tests were performed, and showed that the water content affected the temperature at which the denaturation peak occurred[11]. Dry samples exhibited a denaturation peak at 73.29 ± 4.60 ºC, whereas for samples with 50% water content such a peak was observed at 109.88 ± 0.61 ºC. The study also showed that the temperature at which denaturation occurred increased with the water content of the specimens.

As a result of its complex structure, the scales mechanical response is expected to vary from the external surface to the interior. Micro- and nanoindentation techniques offer the possibility to scan the response both in terms of elastic modulus and hardness[12]. Lin *et al*. carried out micro-indentation tests and found that the hardness of the external layer of the scale was considerably greater than that of the internal layer, consistent with its higher degree of mineralization[13-14].

Here, the structure-mechanical property relation is investigated through the scale of *Arapaima Gigas* that presents gradient properties from its external side to the inside.

2. EXPERIMENTAL

2.1 Materials

Commercially available hatchery-raised *Arapaima Gigas* (body weight 100-150 kg) fish were used. Scales were removed from the main body, washed and stored in standard conditions (20 ºC and 80% of relative humidity). They were around 70-75 mm in length and 1 mm thick.

2.2 Characterization Techniques

2.2.1 Morphological Characterization

Transmission electron microscopy (TEM) was carried out in a Jeol JEM-1010 microscope. The samples were washed with distilled water and immersed 2 h in 0.1 M phosphate buffer and 2% OsO_4 solution at room temperature for fixation. The fixed samples were dehydrated in a series of solutions of 50, 60, 79 and 100% vol. of ethanol concentrations, and then embedded in a polar monomer polyhydroxylated achromatic acrylic resin (LR white resin) and cured at 60 ºC. A Leica UC6 ultra-microtome with diamond knife was used to cut ultra-thin sections of the scales.

2.2.2 Thermogravimetry

Thermogravimetric analysis (TGA) was performed by using a Perkin Elmer TGA4000 Thermogravimetric Analyzer. Powder samples weighing approximately 10-15 mg were analyzed at a heating rate of 10 °C/min from 30 to 800 °C under a nitrogen flow of 20 mL/min. The temperatures at the maximum degradation rate were obtained from derivative thermogravimetric (DTG) curves. The specimens were carefully taken from the inner and outer surfaces of the fish scales in order to compare the mineral contents in those regions.

2.2.3 Nanoindentation

Scale cross sections were cut in sizes ranging from 3 to 5 mm and were mounted in acrylic resin stubs. Then, the mounted samples were progressively polished to finish the surface with a ¼ μm diamond paste using standard polishing equipment. They were deformed by a Berkovich diamond pyramid (tip radius about 380 nm) and observed optically using a Nanohardness tester (NHT) machine from CSEM (Switzerland). The tests were performed in the force-control mode of the machine. The calibration procedure suggested by Oliver and Pharr[15] was used to correct for the load-frame compliance of the apparatus and the imperfect shape of the indenter tip. Indentation lines were made using a maximum load F_m of 2 mN (30 s loading, 30 s hold, 30 s unloading) and a spacing of 5 μm along a direction inclined by about 25° to the scale normal. The load–penetration curves were analyzed using the method proposed by Oliver and Pharr[15]. Hardness corresponds to the mean pressure over the contact area A_c and was calculated as:

$$H = F_m / A_c \tag{1}$$

On the other hand, the composite modulus (specimen–tip) E^* was extracted from the contact stiffness S that is the slope of the unloading curve at maximum penetration:

$$S = \frac{\partial F}{\partial H} = 2\beta E^* \sqrt{\frac{A_c}{\pi}} \tag{2}$$

where β is a correcting factor depending on the tip geometry (β = 1.034 for a Berkovich tip). The composite modulus (specimen–tip) E^* was defined as:

$$\frac{1}{E^*} = \frac{1-\nu_D^2}{E_D} + \frac{1-\nu_S^2}{E_S} \tag{3}$$

where E and ν are Young's modulus and Poisson's ratio, and subscripts D and S indicate diamond and specimen respectively (E_D = 1141 GPa, ν_D = 0.07). The reduced modulus is defined as:

$$\frac{1}{E_r} = \frac{1-\nu_S^2}{E_S} \tag{4}$$

3. RESULTS AND DISCUSSION

3.1 Structural Gradient

Figure 1 shows a cross sectional optical view of the scale with corrugated external layer and subsequent inner layers mostly parallel. The outer part of the fish scale in **Figure 1** is depicted at the most left part of the image. The rough surface of such a layer corresponds to the ridge structure of the fish scale surface. Alternate layers can be observed as light and dark layers. Both light and dark layers become thinner in the inner part of the scales (**Figure 1**). Image analysis was used to measure the thickness of such layers. The thickness of the dark layers in **Figure 1** ranges from 40 to 100 μm whereas the thickness of the light layers ranges from 25 to 50 μm.

Figure 2 shows a TEM micrograph and confirms the plywood-like pattern of the inner layers. Collagen layers are formed by collagen fibres co-aligned within each individual layer. These layers alternatively rotate at angles of around 90° between each layer.

TGA reveals an important change in mineral content between outer and inner surfaces. TGA graphs depicted in **Figure 3**, show that the region close to the outer surface presents a mineral content of about 71 wt.%, whereas the inner surface shows a lower mineral content of 17 wt.%. This is in agreement with the EDX results presented elsewhere[13] in which, the external region of the cross section of *Arapaima Gigas* scales depicts a more pronounced calcium peak for the external layer with regard to the EDX spectrum of the internal layer. According to Lin *et al.*[13], this difference suggests that the external layer has a higher degree of mineralization.

3.2 Mechanical Gradient

Figure 4 shows the mechanical profiles as obtained from the nanoindentation tests on a cross section of a scale (**Figure 1**). It is first observed that important changes take place as depth increases either in terms of elasticity or permanent deformation. Both hardness and reduced modulus are reduced by a factor of three when moving from the external layer to the interior. Noticeably, the scale local response changes gradually to less stiff and less hard. Scatter in mechanical response is observed in such biological materials[14]. Surface preparation is crucial while the mechanical contrast complicates the polishing.

The higher elastic and plastic resistances found in the outer surface of the scale with regard to the lower ones found for the inner surface can be explained if we consider that the scale does not have a constant mineral content across its thickness as revealed above by TGA (**Figure 3**). This confirms that higher mineral contents correspond to harder and stiffer nanocomposite materials. According to Meyers *et al.*[16], the content of the mineral component of *Arapaima Gigas* fish scales decreases as layers are closer to the inner part of the scales. The lower hardness and reduced modulus values would be related to the lower mineral content. The mineral phase of AG scales is formed by calcium deficient hydroxyapatite (HA) platelets with a thickness of ~50 nm and a diameter of ~500 nm. These nano-platelets act as a reinforcement phase. In a previous study, the volume fraction of the HA platelets was estimated to be 21.5%[10].

These results indicate that the fish scale cannot be treated as a uniform and homogeneous laminate structure, as has been treated in the past[3,4]. By contrast, it presents different modifications, both in its organization, as well as in its chemical structure, that allow for the fulfilment of all its functions.

Figure 1. Optical micrograph of an *Arapaima Gigas* scale in cross section (white bar is 100 μm long)

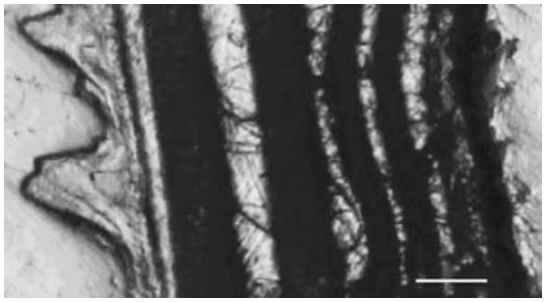

Figure 2. TEM micrographs of an *Arapaima Gigas* scale (black bar is 10 μm long). At high magnification, co-aligned collagen fibres are observed

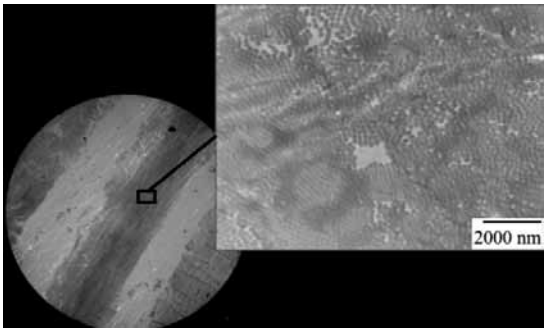

However, the decrease in properties is not steady but follows a cyclic saw-tooth shaped pattern. The peaks of these saw-tooth shaped curves are located inside the layers that appear dark in **Figure 1**, which in fact correspond to the laminates where fibres are perpendicular to the indentation plane.

Figure 4 indicates that the reduced modulus measured using nanoindentation tests has much higher values of 5-30 GPa (humidity of about 15%) than those obtained from tensile tests in a previous study (1.38 GPa, dry state[10]). The reduced modulus E_r is calculated by amplifying the Young´s modulus by a factor $1/(1-\nu^2)$. If we consider a Poisson value of 0.5, then E_r should be 1.33 times the Young´s modulus. However, the increase in reduced modulus measured by indentation techniques, relative to the theoretical estimates, is much higher. Firstly, it is important to point out that the indentation techniques capture in more detail the specific micromechanical properties of the scale, making the effect of the extreme hardness and modulus of the outer layer more noticeable, whereas tensile tests only capture average mechanical properties. Secondly, biological materials containing collagen are known to be strain-rate sensitive. Their elastic modulus evolution with strain rate $\dot{\varepsilon}$ can be written as[13]:

$$E = C|(\dot{\varepsilon})|^n \quad (5)$$

The strain-rate sensitivity n is amplified with hydration and collagen content[13]. During an indentation test with a self-similar Berkovich tip, the strain rate $\dot{\varepsilon}$ is not constant but varies strongly with depth h. Assuming a perfectly sharp tip (no tip rounding) it changes from infinite (at the beginning of the deformation) to zero (at the end) during the experiment[17]:

$$\dot{\varepsilon} = \frac{\dot{h}}{h} \quad (6)$$

However, the average indentation strain rate over the loading ramp can be roughly estimated to about $3x10^{-2}$ s^{-1} while tensile tests were conducted at a rate of $3x10^{-3}$ s^{-1} [10]. Taking a strain rate sensitivity of n = 0.26 [13], a factor of about 1.8 is expected between results carried out at low and high strain rates. Finally, taking into account the $1/(1-\nu^2)$ factor, one obtains a factor of about 2.3 between results for both experimental approaches, while the ratio between modulus of the inside of the scale and the tensile test one is about 3.6.

Figure 3. TGA curves for the (a) outer surface, (b) inner surface of fish scale

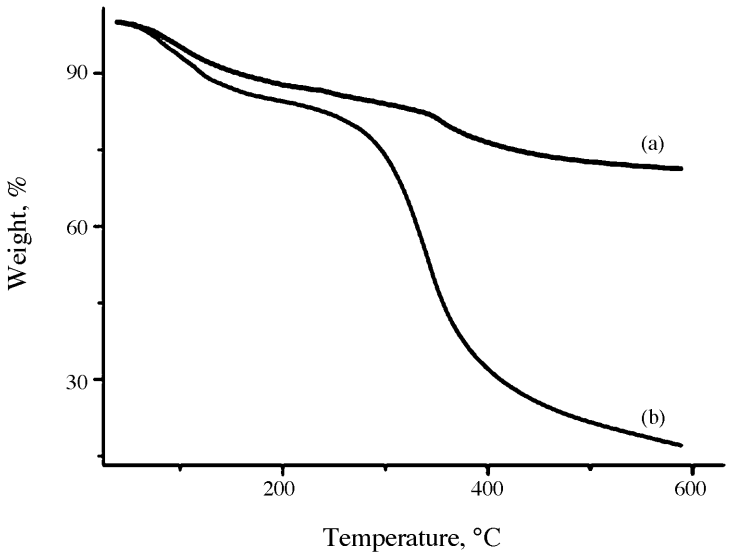

4. CONCLUSIONS

Both the structure and the mechanical response have been scrutinized throughout samples of *Arapaima Gigas* scale. A correlation between mechanical properties and the mineral content has been found. The external layers are mineral rich, hard and stiff. The inside of the scale show a

Figure 4. Hardness (a) and reduced modulus (b) profiles (Depth null corresponds to the external surface)

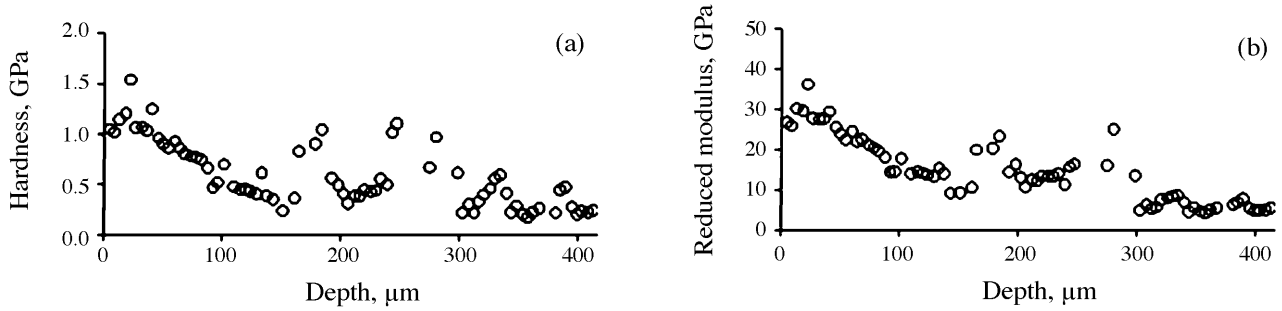

progressive decrease of mechanical properties, with local variations attributed to the plywood structure of the scale. The inner surface, being collagen-rich, is also less hard and less stiff.

ACKNOWLEDGEMENTS

The authors would like to thank the Vicerectorate of Research (VRI) of the Pontificia Universidad Catolica del Peru (PUCP) and the "Consejo Nacional de Ciencia Tecnologia e Innovacion Tecnologica (CONCYTEC)" for financial support.

REFERENCES

1. Sir J.Y. and Akimenko M.A., *Int. J. Dev. Biol.,* **48** (2004) 233.
2. Vernerey F.J. and Barthelat F., *Int. J. Solids Struct.,* **47** (2010) 2268.
3. Zhu D., Ortega C.F., Motamedi R., Szewciw L., Vernerey F., and Barthelat F., *Adv. Eng. Mater.,* **14** (2012) B185.
4. Currey J.D., *J. Exp. Biol.,* **202** (1999) 3285.
5. Sudo S., Tsuyuki K., Ito Y., and Ikohagi T., *JSME Int. J.,* **C 45** (2002) 1100.
6. Browning A., Ortiz C., and Boyce M.C., *J. Mech. Behav. Biomed. Mater.,* **19** (2013) 75.
7. Ikoma T., Kobayashi H., Tanaka J., Wals D., and Mann S., *J. Struct. Biol.,* **142** (2003) 327.
8. Marino Cugno Garrano A., La Rosa G., Zhang D., Niu L.-N., Tay F.R., Majd H., and Arola D., *J. Mech. Behav. Biomed. Mater.,* **7** (2012) 17.
9. Allison P.G., Chandler M.Q., Rodriguez R.I., Williams B.A., Moser R.D., Weiss Jr, C.A., Poda A.R., Lafferty B.J., Kennedy A.J., Seiter J.M., Hodo W.D., and Cook R.F., *Acta Biomater.,* **9** (2013) 5289.
10. Torres F.G., Troncoso O.P., Nakamatsu J., Grande C.J., and Gomez C.M., *Mater. Sci. Eng.,* **C28** (2008) 1276.
11. Torres F.G., Troncoso O.P., and Amaya E., *Mater. Sci. Eng.,* **C32** (2012) 2214.
12. Le Bourhis E., Glass Mechanics and Technology, Wiley, Weinheim (2008).
13. Lin Y.S., Wei C.T., Olevsky E.A., and Meyers M.A., *J. Mech. Behav. Biomed. Mater.,* **4** (2011) 1145.
14. Chen P.Y., Schirer J., Simpson A., Nay R., Lin Y.S., Yang W., Lopez M.I., Li J., Olevsky E.A., and Meyers M.A., *J. Mater. Res.,* **27** (2012) 100.
15. Oliver W.C. and Pharr G.M., *J. Mater. Res.,* **7** (1992) 1564.
16. Meyers M.A., Lin Y.S., Olevsky E.A., and Chen P.-Y., *Adv. Eng. Mater.,* **14** (2012) B279.
17. Le Bourhis E. and Patriarche G., *Phil. Mag. Lett.,* **79** (1999) 805.